9-1-2017

Axon Determination of Subtype Specific Myelin Ensheathment and Pruning

Erin Dankert
Winona State University

Heather Nelson
Winona State University

Samantha Lang
Winona State University

Madeline Martell
Winona State University

Axon Determination of Subtype Specific Myelin Ensheathment and Pruning

Erin Dankert, Heather Nelson, Samantha Lang, Madeline Martell, A.J. Treichel, Jacob Hines
Biology Department, Winona State University, Winona MN

1. Introduction

In the developing spinal cord, pre-myelinating oligodendrocytes dynamically extend and retract processes within white matter tracts containing numerous distinct axon subtypes. Oligodendrocytes display axon subtype preference and ultimately myelinate some subtypes while leaving others unmyelinated (Figure 1).

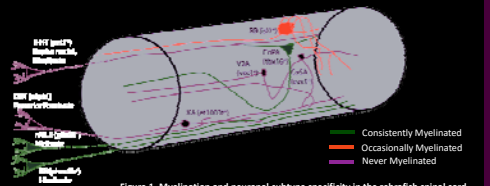

Figure 1. Myelination and neuronal subtype specificity in the zebrafish spinal cord.

A series of distinct cell behaviors precede and initiate selective myelination. Whether sheath initiation, growth, and pruning are determined by oligodendrocytes or properties of individual axons is poorly understood.

In this study we address the following questions:

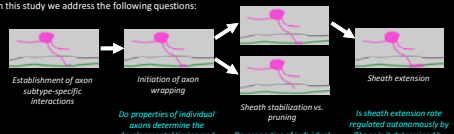

2. Does axon subtype direct order and rate of ensheathment?

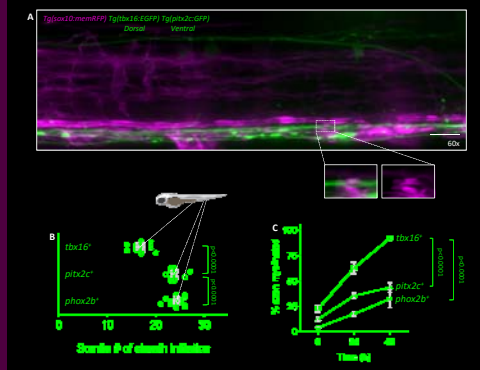

Figure 2. Individual axon subtypes initiate myelination at different time points and proceed with different rates of ensheathment. (A) Representative image shows a posterior segment where myelination has initiated on *pitx2c*$^+$ but not *tbx16*$^+$ axons. Because ensheathment occurs as an anterior to posterior wave, larger somite numbers reflect earlier axon ensheathment. Scale bar is 10 µm. **(B)** Oligodendrocytes initiate myelination of different axon subtypes at non-overlapping developmental time points. n=10 larvae (*tbx16*), 10 (*pitx2c*), 14 (*phox2b*). **(C)** Percentage of total axon length wrapped by *sox10*$^+$ processes at the indicated time point. n=11, 14, and 25 larvae for tbx16 (time points 0, 24, 48h, respectively); n=15, 12, 6 for phox2b; n=11, 11, 18 for pitx2c.

3. Ablation of projection axons by spinal cord injury

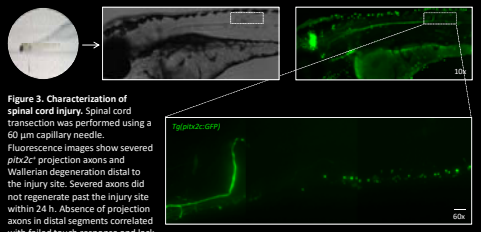

Figure 3. Characterization of spinal cord injury. Spinal cord transection was performed using a 60 µm capillary needle. Fluorescence images show severed *pitx2c*$^+$ projection axons and Wallerian degeneration distal to the injury site. Severed axons did not regenerate past the injury site within 24 h. Absence of projection axons in distal segments correlated with failed touch response and lack of free swim. Scale bar is 10 µm.

4. Does spinal cord injury affect OL abundance in posterior segments?

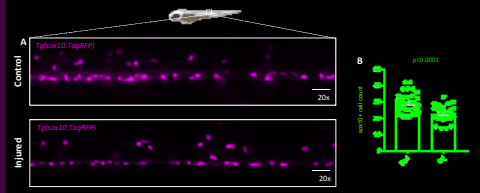

Figure 4. Spinal cord injury marginally reduces OL number in distal segments. (A) Typical distribution and number of OLs 24 hours post-injury (hpi) marked by *Tg(sox10:TagRFP)* in somites 24-26. Scale bar is 25 µm. **(B)** Injury reduced OL number by 22.4% compared to controls. n=33 (control) and 30 (injured).

5. Does reduction of preferred axon subtypes influence myelination?

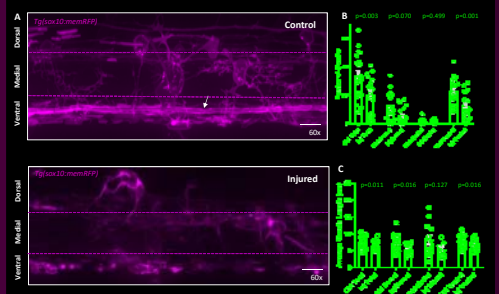

Figure 5. Reduction of preferred axons causes reduces myelination in distal segments. (A) Representative images of myelin sheaths in control and injured larvae. Data were acquired in somites 24 and 25 (ctrl n=22, inj n=19). The Mauthner axon (Fig 5A arrow) was excluded from data. Scale bar is 10 µm. **(B)** Sheath number measurements in spinal cord sub-domains. Note the overall 41% reduction in sheath number in injured animals (B). **(C)** Average sheath length measurements in spinal cord sub-domains.

6. Do individual axon subtypes determine myelin ensheathment rate?

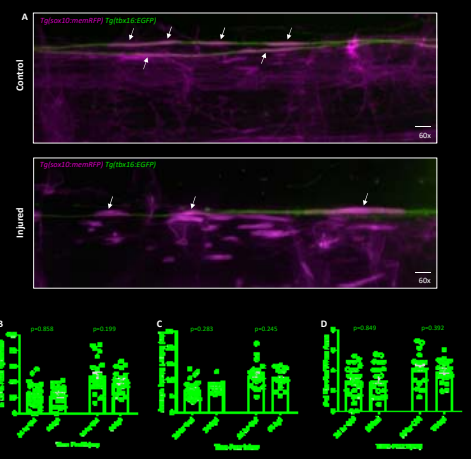

Figure 6. *tbx16+* axons maintain a constant ensheathment rate in an axon-deficient environment. (A) Typical wrapping of the CoPA axon in control (two axons in image) and injured larvae at 24 hpi. Data were acquired in somites 16 and 17 (24 hr ctrl n=35, 24hpi n=22, 36 hr ctrl n=23, 36hpi n= 20). Arrows denote wrapping. Scale bar is 5 µm. **(B)** Percentage of CoPA axon myelinated was unchanged by injury. **(C)** Average sheath length on the CoPA axon was unchanged by injury. **(D)** The number of sheaths per 100 µm of CoPA axon was unchanged by injury.

7. Can oligodendrocytes adaptively shift myelin between axon subtypes?

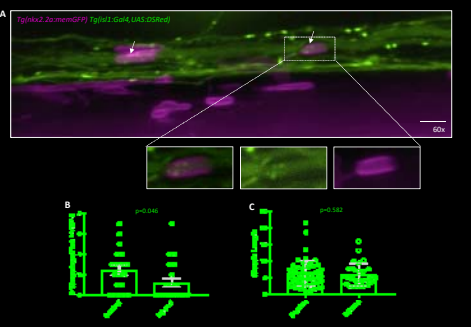

Figure 6. *isl1+* axons maintain minimal ensheathment in an axon-deficient environment. (A) Representative wrapping of the Rohon-Beard sensory axon at 24 hpi. Data were acquired in all somites 21+ (ctrl n=19, inj n=21). Arrows denote wrapping. Scale bar is 5 µm. **(B)** The number of wrappings on the Rohon-Beard axon was significantly decreased by injury. **(C)** Average sheath length on the Rohon-Beard axon was unchanged by injury. Each point represents one sheath.

8. Does axon subtype determine extension and pruning of sheaths?

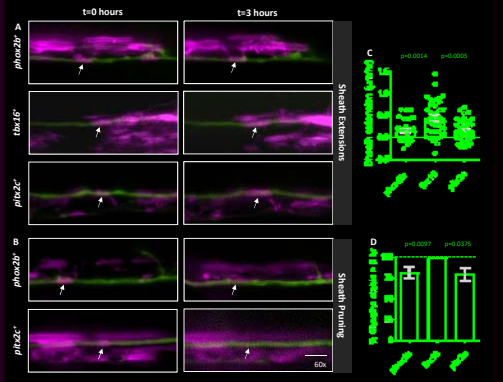

Figure 8. Sheath extension rate and pruning frequency differ between axon subtypes. (A) Sheath extension on a *phox2b*$^+$, *tbx16*$^+$, and *pitx2c*$^+$ axon. Arrows denote wrapping. **(B)** Sheath pruning on a *phox2b*$^+$ and *pitx2c*$^+$ axon. Arrows denote wrapping. Scale bar is 5 µm. **(C)** Sheath extension rates over a period of three hours. Sheaths wrapping *tbx16*$^+$ axons extended faster than those on *pitx2c*$^+$ and *phox2b*$^+$ axons. **(D)** Percentage of sheaths stable over a period of three hours. OLs occasionally pruned sheaths wrapping *pitx2c*$^+$ and *phox2b*$^+$ axons but not *tbx16*$^+$ axons (39/39 sheaths stable). n=27 phox2b$^+$ axons, n=39 tbx16$^+$ axons, n=39 pitx2c$^+$ axons.

9. Conclusions and working models

1. Myelination of distinct neuronal subtypes initiates in a specified order and progresses at different rates
2. Individual axon subtypes control ensheathment rate by regulating both sheath extension rate and pruning frequency
3. (Some) axon subtypes possess autonomous cues maintaining ensheathment fate and rate in an altered environment

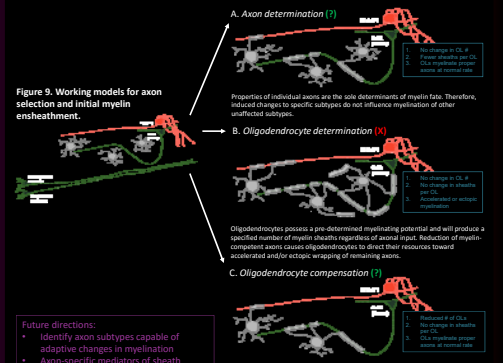

Figure 9. Working models for axon selection and initial myelin ensheathment.

Future directions:
- Identify axon subtypes capable of adaptive changes in myelination
- Axon-specific mediators of sheath extension and pruning

We thank Mark Masino (University of Minnesota), Bruce Appel (University of Colorado), Mary Halloran (Wisconsin), and Michael Lardelli (University of Adelaide) for providing zebrafish lines. This work was funded by Winona State University Foundation Special Project grants 251.0225 and 251.0253 (JH), National Multiple Sclerosis research grant 5274A1/T (JH), and WSU research supply grants (H.N., E.D., A.T., M. K., M.M). We thank The WSU College of Science & Engineering, Biology Department, Ted Wilson, Richard Deyo, and Ed Thompson for supporting instrumentation funds (spinning disk confocal microscope) and Michael Delong for use of incubator.